Pergamon

PII: S0021-9169(96)00061-X

Journal of Atmospheric and Solar-Terrestrial Physics, Vol. 59, No. 8, pp. 853–872, 1997

1364-6826/97 $17.00+0.00

A study of substorm-associated nightside spike events in auroral absorption using imaging riometers at South Pole and Kilpisjärvi

J. K. Hargreaves,[1]* S. Browne,[1] H. Ranta,[2] A. Ranta,[2] T. J. Rosenberg[3] and D. L. Detrick[3]

[1]Engineering Department, University of Lancaster, Bailrigg, Lancaster LA1 4YQ, U.K.; [2]Geophysical Observatory, Sodankylä, SF-99600, Finland; [3]IPST, University of Maryland, College Park, MD 20742, U.S.A.

(*Received in final form* 4 *March* 1996; *accepted* 21 *March* 1996)

Abstract—The short-duration 'spike' events which are a common feature of substorm-associated auroral radio absorption in the midnight sector are observed both at Kilpisjärvi (69.05°N, 20.79°E, $L = 5.9$) in the auroral zone and at the much higher latitude of the South Pole (90.00°S, $L = 13$). These events have been known for many years, but it is only recently, since the evolution of the imaging riometer, that it has become possible to measure their size, shape and movements.

It is found that the spike events are remarkably similar at the two latitudes studied. They are usually elliptical in shape with the major axis generally along rather than across the L shells; median dimensions are 167 km by 74 km at the South Pole, and 190 km by 80 km at Kilpisjärvi. It may be significant that in each case the perturbed region of the ionosphere maps to an almost circular region at the magnetospheric equatorial plane, and that the total magnetic flux included within the event is similar at each latitude. The velocities of the events are variable in the range of several 100 m/s to 2 or 3 km/s; the direction of motion tends to be poleward at the beginning of a precipitation event, and is often equatorward towards the end. The east–west component has not shown any consistency of direction at Kilpisjärvi, though its magnitude may be as large as the north–south one. It is shown that the true duration of a spike event is only 1–2 min.

The effect of the spike event's limited extent on wide-beam measurements is investigated, and it is shown that a typical wide-beam riometer underestimates the absorption by a factor of 2 to 3 for spikes occurring at the onset of a substorm. This does not necessarily apply to the later phases of the substorm when the precipitation is likely to be more widespread.

The slowly moving absorption bay which may precede the intense precipitation at substorm onset has been detected over Kilpisjärvi. It is identified as an arc-like feature extending east–west across the entire field of view, but containing structure. Its typical north–south extent is 60–100 km, and its equatorward speed is a little over 100 m/s.

1. THE SPIKE EVENT IN AURORAL RADIO ABSORPTION

The 'spike event' was first studied by Parthasarathy and Berkey (1965) though that name was not applied to it until some years later. The spike is easily recognized in riometer data because of its sudden beginning, short duration and moderately high intensity. It is of special interest in relation to substorm mechanisms and effects, since most spikes occur at or near the start of a substorm-related precipitation event in the midnight sector. It is thus one of the first effects to be registered on ground-based equipment when a substorm occurs in the magnetosphere.

More recently, Stauning and Rosenberg (1995) have reported on daytime high latitude absorption spike events. These daytime events appear to be a population quite distinct from those, studied here, that occur on the nightside during substorms. The daytime spikes have similar durations of 1–2 min, but in contrast are weak (typically 0.2–0.3 dB), somewhat smaller in extent and show little evidence of motion. Nevertheless, similar mechanisms may be responsible for the generation of spiky absorption in both cases.

The diurnal occurrence of spike events at Abisko ($L = 5.6$), which is in the Scandinavian sector and not too far from Kilpisjärvi, is given in Fig. 1. The distribution peaks a little before magnetic midnight, and half the events occur within a 3 h period. Examples of spike events observed with a wide-beam riometer at Kilpisjärvi, are shown in Fig. 2.

Using a narrow-beam riometer at Ramfjordmoen ($L = 6.2$), Nielsen and Axford (1977) first demonstrated spike events that were only several 10s of km wide in the north–south direction, and were therefore narrower than the beam of a standard riometer of that

*Formerly with Environmental Sciences Dept.

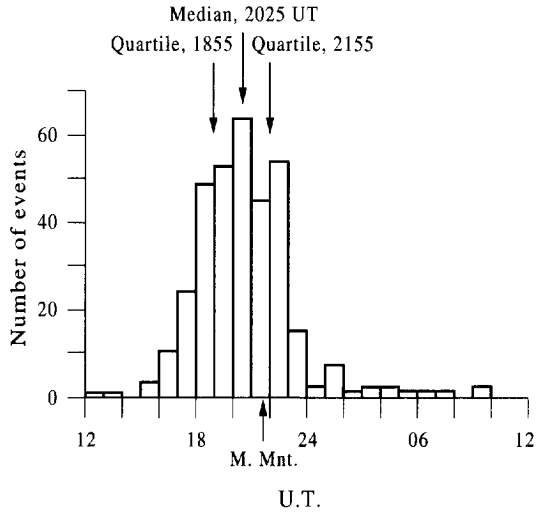

Fig. 1. Occurrence of spike events (1 dB) at Abisko, 1980–1985 (after Taylor, 1986). Abisko is in the same time sector as Kilpisjärvi and at a similar L value. Magnetic midnight is about 2130 UT.

time projected to the 90 km level. It was assumed that the events were very extended in the east–west plane. This was an observation of some significance for riometry, demonstrating that at least one type of event has spatial structure smaller than had hitherto been thought. Hargreaves *et al.* (1979) verified the narrow extent by comparing measurements with wide and narrow beams, and with wide-beam riometers on different frequencies; they estimated widths of 36 km at the South Pole and 72 km at Ramfjordmoen, between points $e^{-1/2}$ ($= 0.61$) of the maximum assuming a Gaussian cross-section. This work assumed that the event was in the form of an east–west strip, and that its apparently short duration was due to rapid motion across the observing beam. (As we shall see, both of these assumptions were false.)

2. THE IMAGING RIOMETERS AT THE SOUTH POLE AND KILPISJÄRVI

The first 'imaging riometer' worthy of the name was installed at the South Pole station by the Institute for Physical Science and Technology of the University of Maryland, U.S.A. Development of the concept* and the hardware had begun in 1984, and the installation was made during the austral summer of 1987–1988. The system operates at 38.2 MHz, and uses an array of 64 crossed half-wave dipoles over a ground plane, with a set of Butler matrices to form 49 independent beams. (The phasing is such as to place one beam directly overhead, and there are a further 15 beams pointing along the ground which are not used.) The signals are received by time sharing into 7 riometers, the outputs of which are digitized (8 bits) every second. The basic time resolution of the system is thus 1 s. The narrowest beam (zenithal) is 13 degrees wide between half-power points, and the best spatial resolution at 90 km (overhead) is about 20 km. The oblique beams are considerably wider. A view of the coverage at the 90 km level is shown in Fig. 3. A detailed description of the South Pole IRIS (Imaging Riometer for Ionospheric Studies) has been given by Detrick and Rosenberg (1990).

The system at Kilpisjärvi also operates at 38.2 MHz and is very similar to that at the South Pole. The riometers have receiver boards of new design, timing is by GPS reception, and digitization is 12 bit instead of 8 bit. Except for improved lightning protection, the antennas, ground plane, and Butler matrix assembly are as in the original Maryland design. The eighth riometer, which at the Pole is held as a spare, is here connected to a wide-beam antenna at the site. The output from the wide-beam instrument is used for quick-look purposes. The system was installed at Kilpisjärvi during August 1994 by the Engineering Department of the University of Lancaster, England, with the active support of the Geophysical Observatory at Sodankylä, Finland. This system is aligned geographically north–south.

*The idea of using Butler matrices to form several beams simultaneously in a riometer system was prompted by a technique used in interplanetary scintillation experiments at the University of California at San Diego, and was first brought to the attention of the riometer community in the early 1970s by Dr. H. J. A. Chivers.

3. SPATIAL DIMENSIONS OF SPIKE EVENTS

3.1. *An example from Kilpisjärvi*

The colour plot of Fig. 4 illustrates typical behaviour of a spike at Kilpisjärvi. Each panel covers a 240 km square at the 90 km level, and the images are 10 s apart. These plots (and all others in this article) are made as if looking down on the D region from above; north is to the top and east is to the right. Note the sudden appearance of the event, in a restricted region; its generally poleward motion, accompanied by some east–west movements; the fading of the event after 50 s, though it remains in view at lower intensity for a further 3 min.

In this example the most intense region passed through the field of view from south to north (i.e. poleward) in about 4 min. Some panels show an arc-

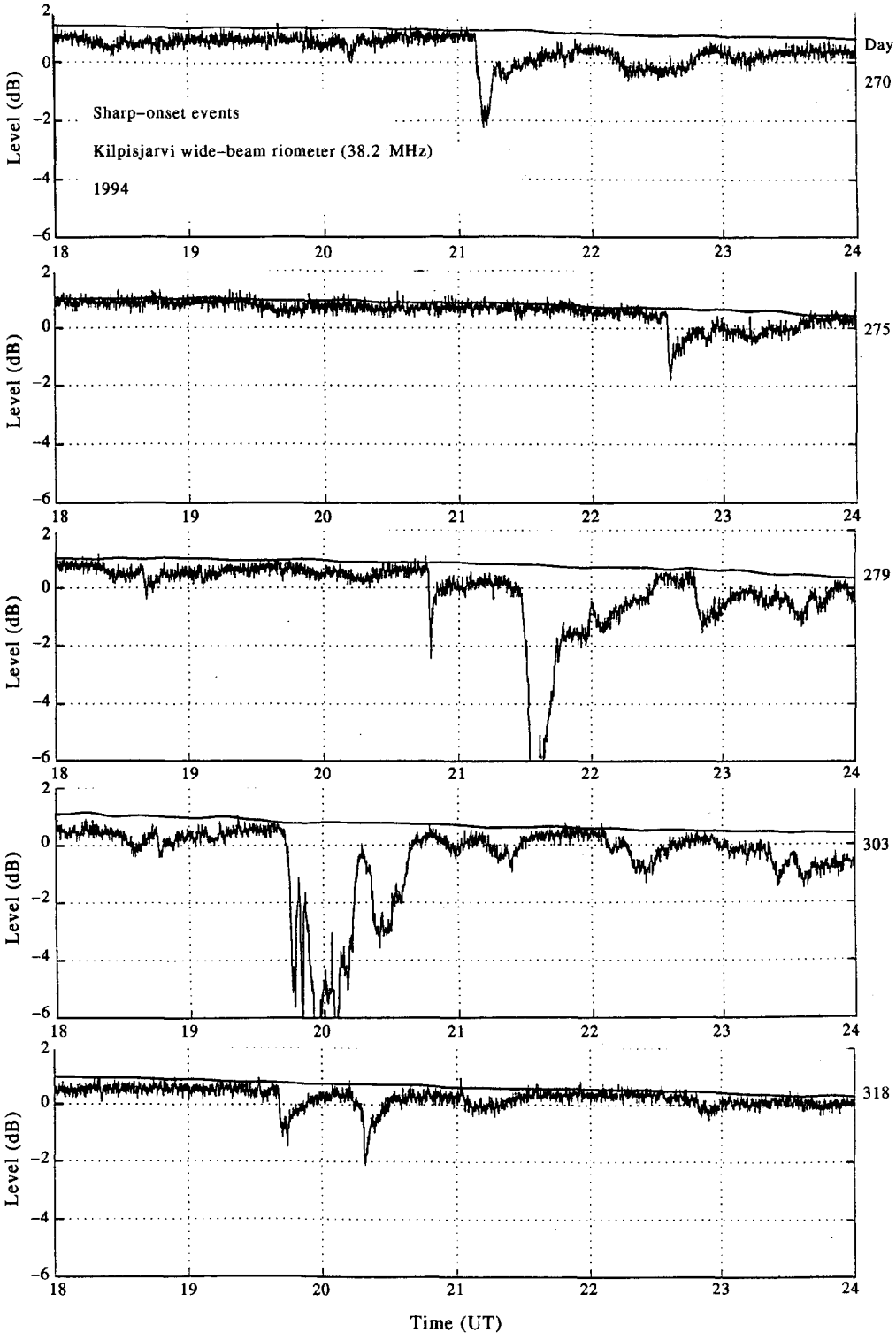

Fig. 2. Examples of sharp-onset events observed with the 38.2 MHz wide-beam riometer at Kilpisjärvi on 5 separate days in 1994. The dates are 27 September (day 270), 2 October (day 275), 6 October (day 279), 30 October (day 303) and 14 November (day 318).

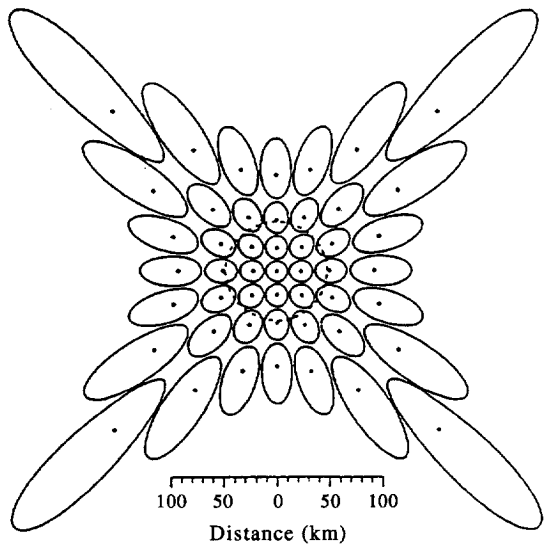

Fig. 3. Projection of the IRIS beams at 90 km altitude (Detrick and Rosenberg, 1990). The beam centres are marked as dots, and the 3 dB levels as solid lines. The dashed circle is the projection of a typical wide-beam riometer antenna.

like structure, and it is tempting to see the intense event as a brightening within that arc. The shape of the event changes, but its most common form is neither circular nor arc-like but as a blob with generally east–west elongation which we shall treat as an ellipse. Whereas there is no detectable absorption before the event, the later panels (which are dark blue in colour rather than black) indicate that more widespread precipitation has followed the spike event up from the south.

3.2. *Event dimensions at Kilpisjärvi*

The events were measured from contour plots such as Fig. 5, which presents a number of examples from Kilpisjärvi. Each shows an enhancement with approximately east–west elongation. Most are also consistent with the presence of a weak arc at about the 0.5 dB level, though this is perhaps not clear enough to constitute proof. The dimensions and orientation were measured by regarding each contour plot as an ellipse. The major and minor axes were measured between absorption values half those of the maximum, and the tilt was estimated from the line of the major axis with respect to east–west.

Table 1 lists the dimensions of 10 such spike events. All major axes exceed 100 km, and all but one minor axes are smaller than 100 km. Typical axial ratios are 2 to 3, and the orientations are plainly east–west rather than north–south. The histograms of Fig. 6 summarize the statistics. Median values are 190 km for the major axis, 80 km for the minor axis, and 2.5 for the axial ratio.

3.3. *Event dimensions at the South Pole*

The selection of night events at Pole was taken from 1988 and 1989. Some properties of the 1988 events were reported by Hargreaves *et al.* (1991). The data set was extended partly to verify the earlier results, but also to provide a stronger base for comparison with the new data from Kilpisjärvi. In all 42 sharp peaks were examined from 7 events lasting between 15 and 60 min. These fell within the early part of the group of night-time events as determined by Hargreaves *et al.* (1964). They yielded 28 measurements of axial dimensions (the remainder being too poorly defined or not sufficiently within the field of view). An orientation angle was measured from 21 examples. The statistics of the dimensions are summarized in Fig. 7. The median major and minor axes are 167 km and 74 km respectively, and the median axial ratio is 2.4. The latter is taken over values greater than 1.5; it comes down to 2.3 if all values are included.

Table 1. Dimension of spike events

Day	Point	Major axis (km)	Minor axis (km)	Axial ratio	Tilt (°)
252	35	110	96	1.1	—
270	49	114	46	2.5	−10
275	33	180	57	3.2	−40
279	42	171	74	2.3	−30
280	164	200	64	3.1	+30
303	102	238	141	1.7	—
	121	246	97	2.5	+18
305	59	192	94	2.0	−3
318	67	192	81	2.4	−11
	293	186	73	2.6	+21

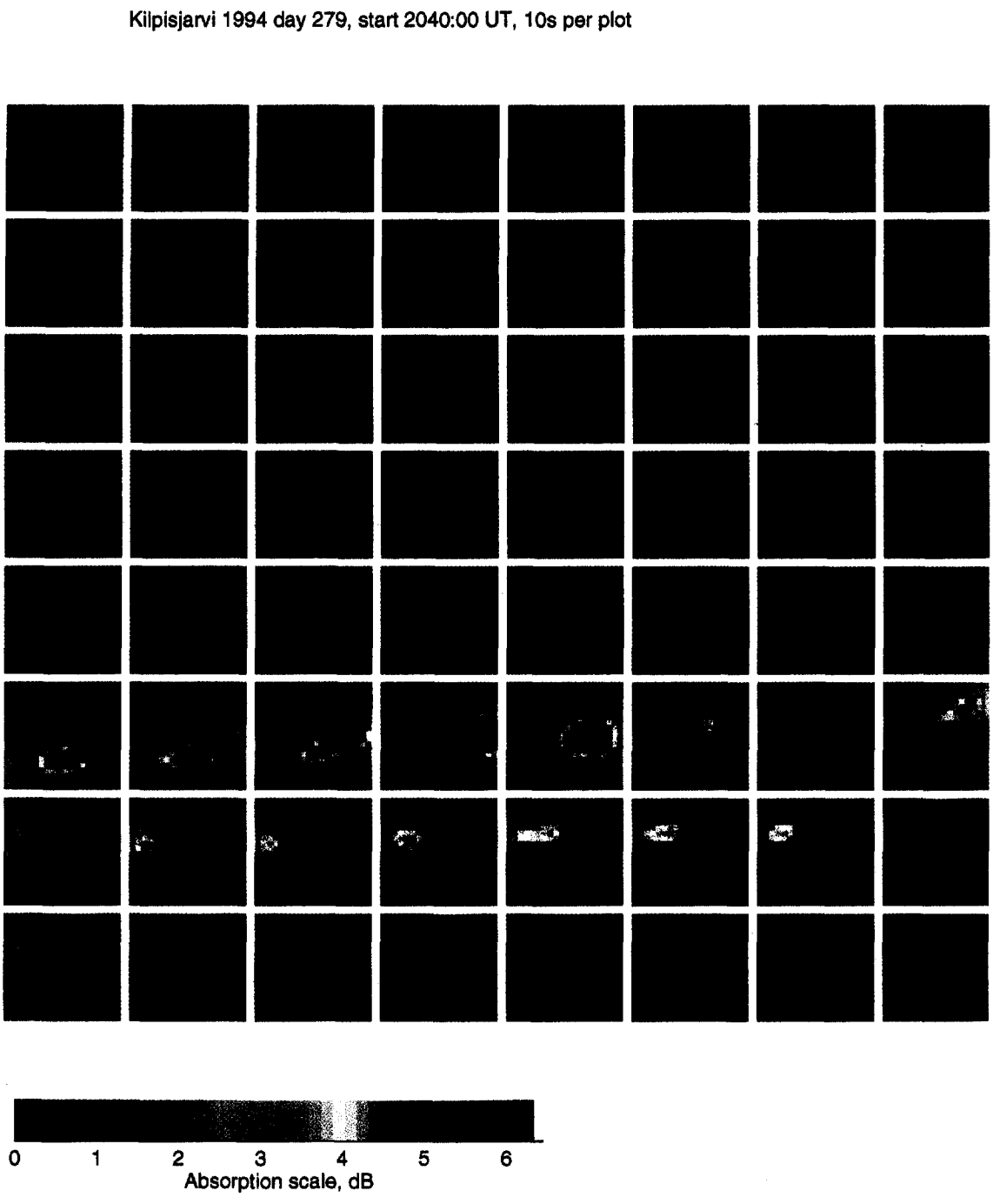

Fig. 4. Example of a spike event at Kilpisjärvi, day 279 (6 Oct 1994). The pictures are 10 s apart and each is 240 km on the side (at the 90 km level). This example shows the elongation of the event, the limited duration of the brightening, and the overall poleward motion.

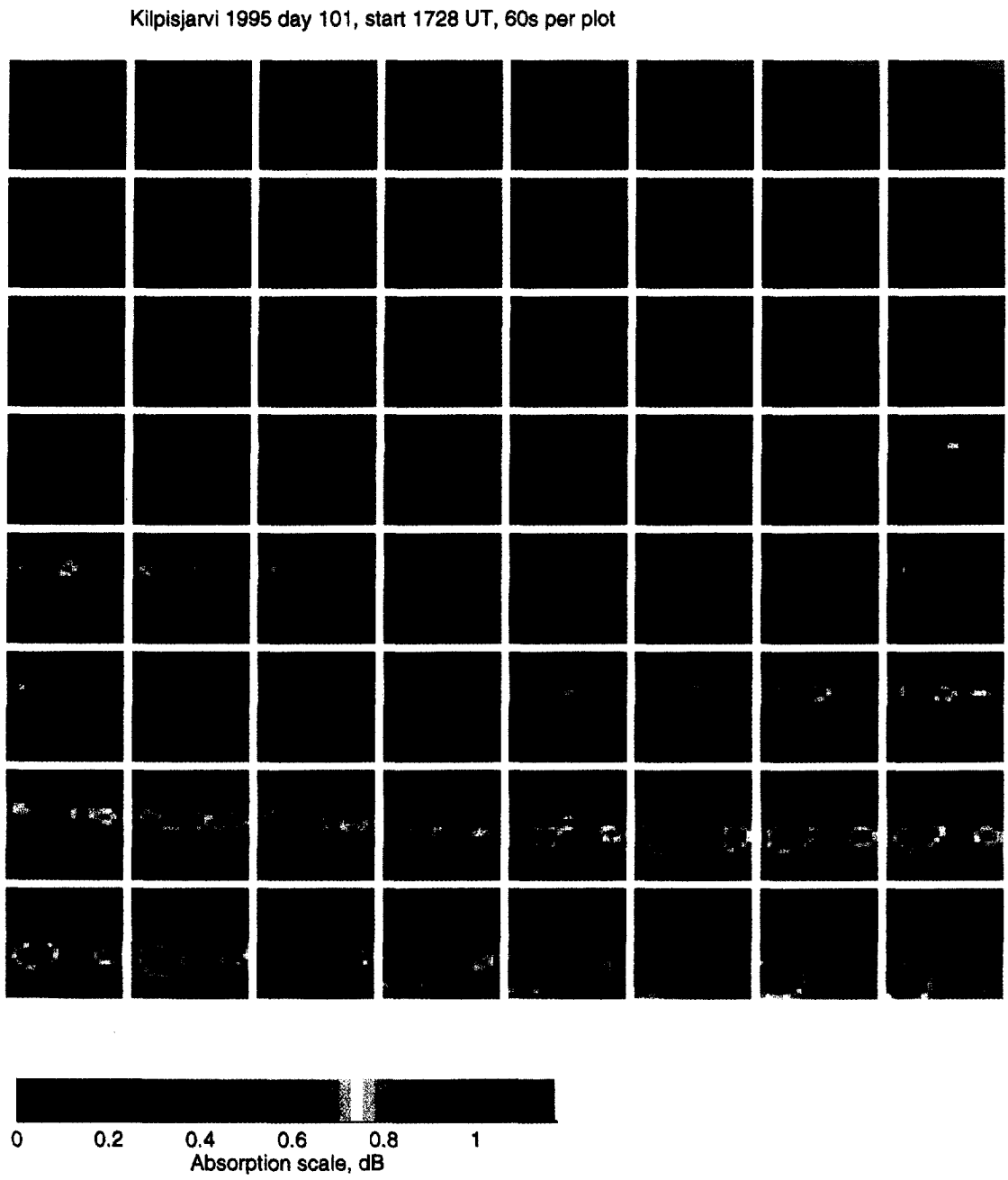

Fig. 19. Equatorward progression of pre-onset bay on day 101, 11 April 1995. There is one picture per minute, starting at 1728 UT. The bay took more than an hour to move across the field of view.

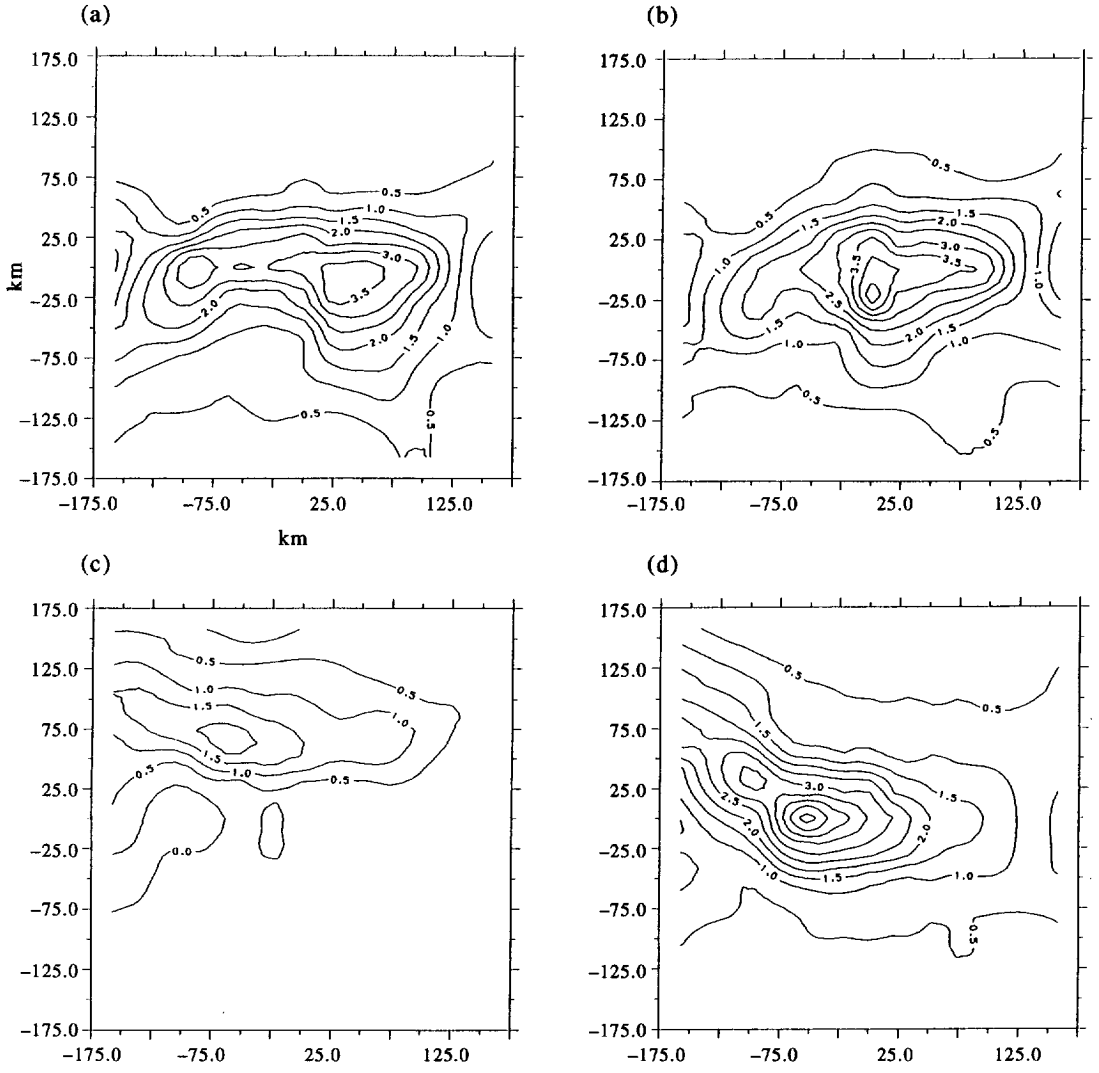

Fig. 5. Contour plots of selected spike events at Kilpisjärvi. The distances are in km (at the 90 km level) and the absorption contours are in decibels. The dates and times are as follows. (a) 1 November, 2239:30 UT (day 305, point 58); (b) 1 November, 2239:40 UT (day 305, point 59); (c) 14 November, 2015:10 UT (day 318, point 272); (d) 14 November 2018:40 UT (day 318, point 293). The maximum absorption ranges between 2 dB (c) and 5 dB (d).

3.4. *Comparison and significance*

The remarkable fact about the spatial sizes of the spike events at the two sites is their similarity. They are being observed at quite different magnetic latitudes, the respective L values being 5.9 and 13, and their intensities are quite different, the typical Kilpisjärvi events being several times larger (in decibels) than those at the Pole. Table 2 makes some comparisons. The axial ratios are almost the same, and the areas covered within the half-absorption contours differ by less than 25% (assuming the elliptical form) on average. Assuming a dipole field, the patches project to almost (within 30%) circular regions at the magnetospheric equatorial plane. Although these patches are different in size, the total magnetic flux which they contain is the same to about 15% on average.

It is obvious that the events detected at such widely separated stations cannot be one and the same, as the event is seen to grow and decay well within the field of view of the imaging riometer (< 300 km) – as illustrated in Fig. 4. Nevertheless, it does seem that the

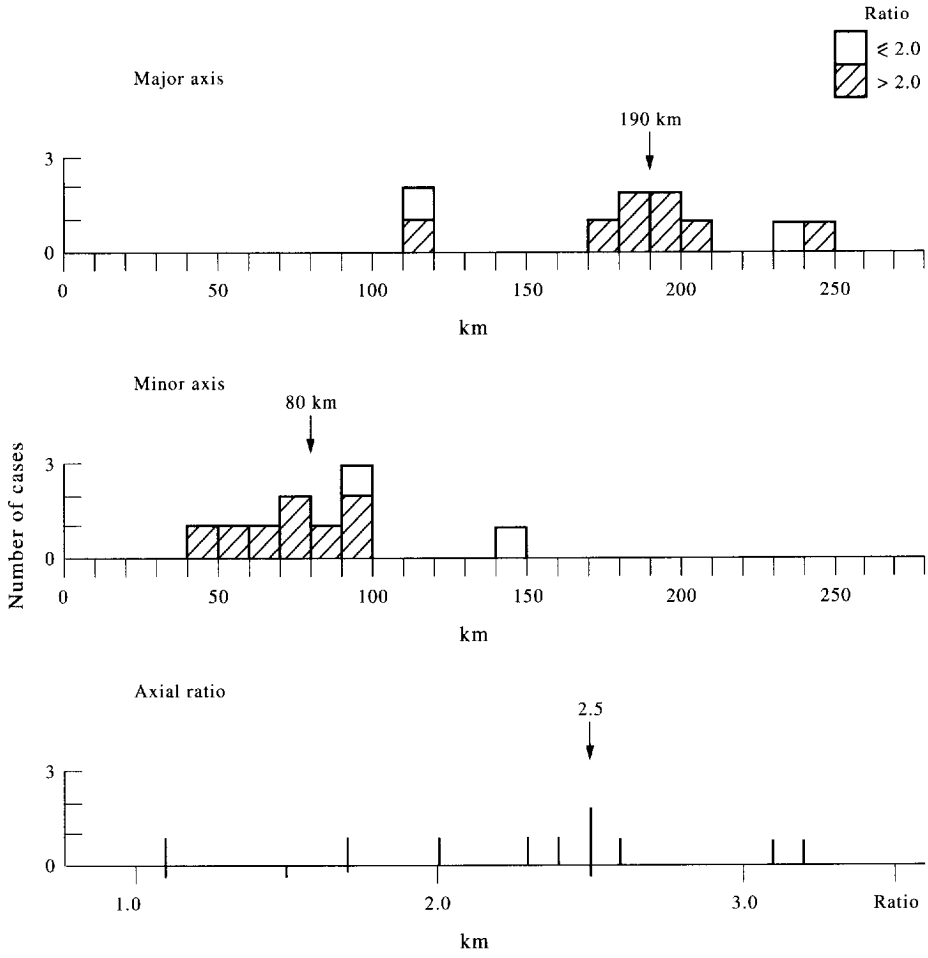

Fig. 6. Statistics of the dimensions of night-time spike events at Kilpisjärvi.

Table 2. Comparison between sizes of events at Kilpisjärvi and the South Pole

	Kilpisjärvi	South Pole
Major axis	190 km	167 km
Minor axis	80 km	74 km
Ratio	2.5	2.4
Area	11,940 km^2	9700 km^2
Major axis projected to equatorial plane	2717 km	7832 km
Minor axis projected to equatorial plane	2088 km	6667 km
Ratio	1.3	1.2
Flux density	1.51×10^{-7} Wb/m^2	1.41×10^{-8} Wb/m^2
Total flux in event area	8.57×10^5 Wb	7.36×10^5 Wb

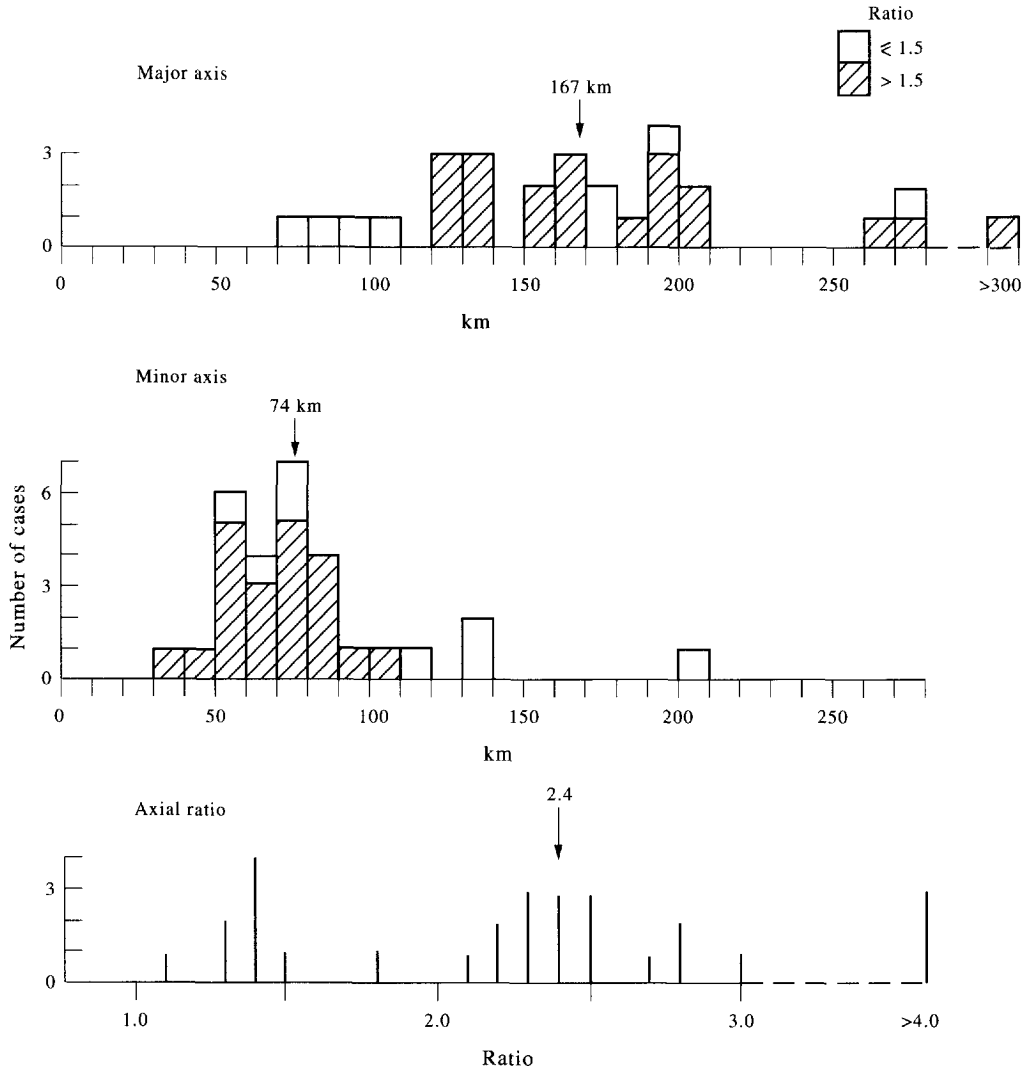

Fig. 7. Statistics of the dimensions of short night-time events at the South Pole. The distribution of axial ratio appears to be bimodal. The median ratio is 2.4 if taken over values $\geqslant 1.5$. If all values are included the median is 2.3.

brightening which we observe as a spike event does occupy an area in the D region which is independent of the latitude, and that the total magnetic flux may be the common factor which determines this.

3.5. *Orientation*

Figure 8 compares the orientations of the events at the South Pole and Kilpisjärvi. The angles were measured with respect to the 'east–west' axis of the array in each case. The Pole IRIS was originally oriented to the magnetic south, using a compass, and the local L shell (computed for $L = 13.2$) is 17 degrees anticlockwise. The median orientation of the elliptical spike events is 29 degrees. It may be thought that the measurements are too crude for a difference of only 12 degrees to matter, but with the number of events plotted in the histogram the difference begins to look statistically significant. There is no obvious physical reason for it, however. This does not, of course, affect our broader conclusion that the events are orientated more nearly along the L shells than across them.

The Kilpisjäri IRIS was oriented to true north using surveying techniques. The L shell there is about 10 degrees away from the east–west line, and the median orientation of the spike events is 12 degrees away, but there are too few values for a useful con-

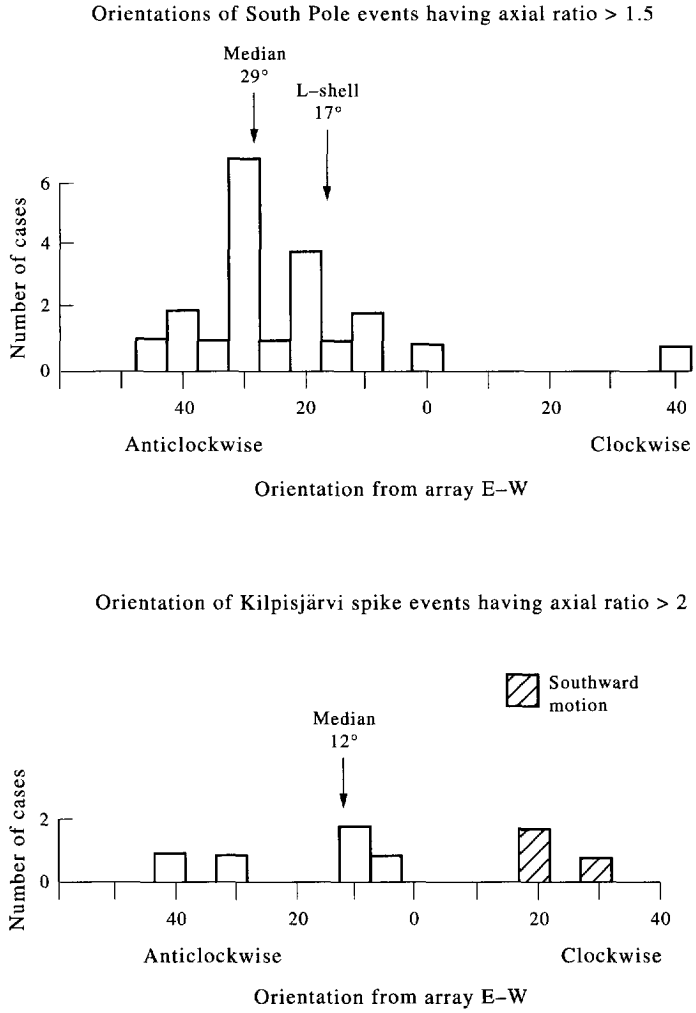

Fig. 8. Statistics of the orientation of events at the South Pole and Kilpisjärvi. At the Pole the median is 12° off the direction of the L shell. At Kilpisjärvi the median is close to the L shell (12°, 10°); the statistics are poor, but there appears to be a distinction according to the direction of motion of the event.

clusion to be drawn (except a broad one as in the paragraph above). However, a further comment will be made in Section 5.3.

3.6. *Some exceptions*

If there is a general rule about the size and shape of auroral-absorption spike events, then it is that they tend to be elliptical in the D region with the typical sizes presented above. However, some of the events certainly do not conform. Some are clearly round rather than elliptical, an example from the South Pole being shown as Fig. 9. This is again plotted to give the view of an observer looking down. South is to the top and east is to the left.

In other cases, and on a finer time scale, there may be detected an alternation of ionization between two regions within the field of view. In Fig. 10, again from the Pole, two regions are seen to intensify at different times, the last state being similar to the first one. These plots are from 1 s data, and the time intervals between successive maps are 8, 8, 14 and 10 s. The whole sequence takes only 40 s.

3.7. *Contraction of the peak*

The foregoing measurements (in Sections 3.2 and 3.3) on the size and shape of spike events have been limited to the time of greatest absorption. But when considering the growth and decay of an event it is of interest to ask whether it intensifies and decays as a whole or whether the dimensions alter. The earlier

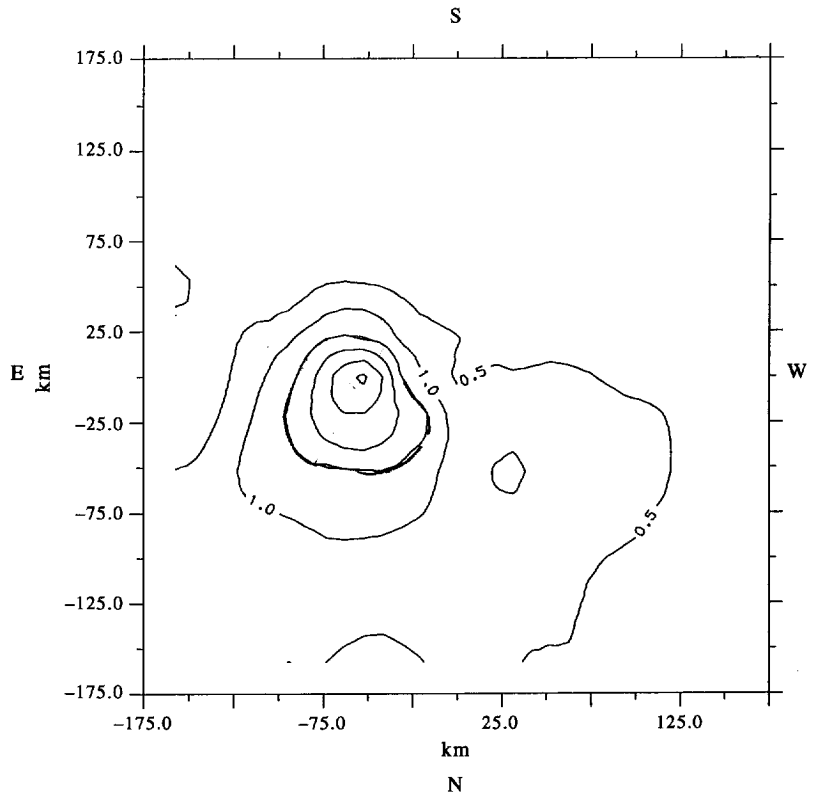

Fig. 9. Example of a round event at the South Pole: 1 April 1989 at 2230:20 UT (Event 89__91, peak 4). The maximum absorption is 3 dB.

report (Hargreaves *et al.*, 1991) showed three examples from the South Pole where in fact the area of the event (defined by the contour of half the maximum absorption) shrank as the event grew in intensity, and then expanded again as the peak decayed. That property has been found to apply also in the later South Pole events, and a clear example is plotted as Fig. 11. Here the area shrinks by approximately a factor of 3 as the peak rises by about the same factor, and there is approximately an inverse relationship. It should be kept in mind that one expects the particle flux to vary with the square of the absorption, other things being equal, so we are not seeing merely a redistribution. However, it appears that the event does become more concentrated as it develops.

4. EFFECT ON THE READING OF A WIDE-BEAM RIOMETER

If the auroral absorption occurs in small patches, which are less than the region covered by the beam of the riometer in the D region, the magnitude of the absorption will be underestimated. Most statistical data on auroral absorption have been compiled from wide-beam instruments, and, though the problem has been well recognized, the means to resolve the issue have not been generally available. At Kilpisjärvi a wide-beam riometer is also operated on the same frequency as the IRIS, and we may therefore compare the wide-beam readings with those from selected narrow beams of the IRIS.

Figure 12 shows an example. The first panel gives the absorption derived from the wide-beam riometer. The next two show the patterns registered by two selected IRIS beams, and the final bottom panel shows the greatest absorption recorded by any beam of the array irrespective of its pointing. (All values are, of course, corrected for obliquity to give an equivalent zenithal absorption value.) Absorption values up to 10 dB are found in beam $(-1, -2)$, compared with about 6 dB in the wide-beam riometer (panel a) during the first part of the event. Some 9 min later, beam (1,1) registered nearly 13 dB, compared with 10 dB in the wide beam. These are intense events, but the tendency seems to be general – that a selected IRIS beam can be found which indicates considerably more absorption

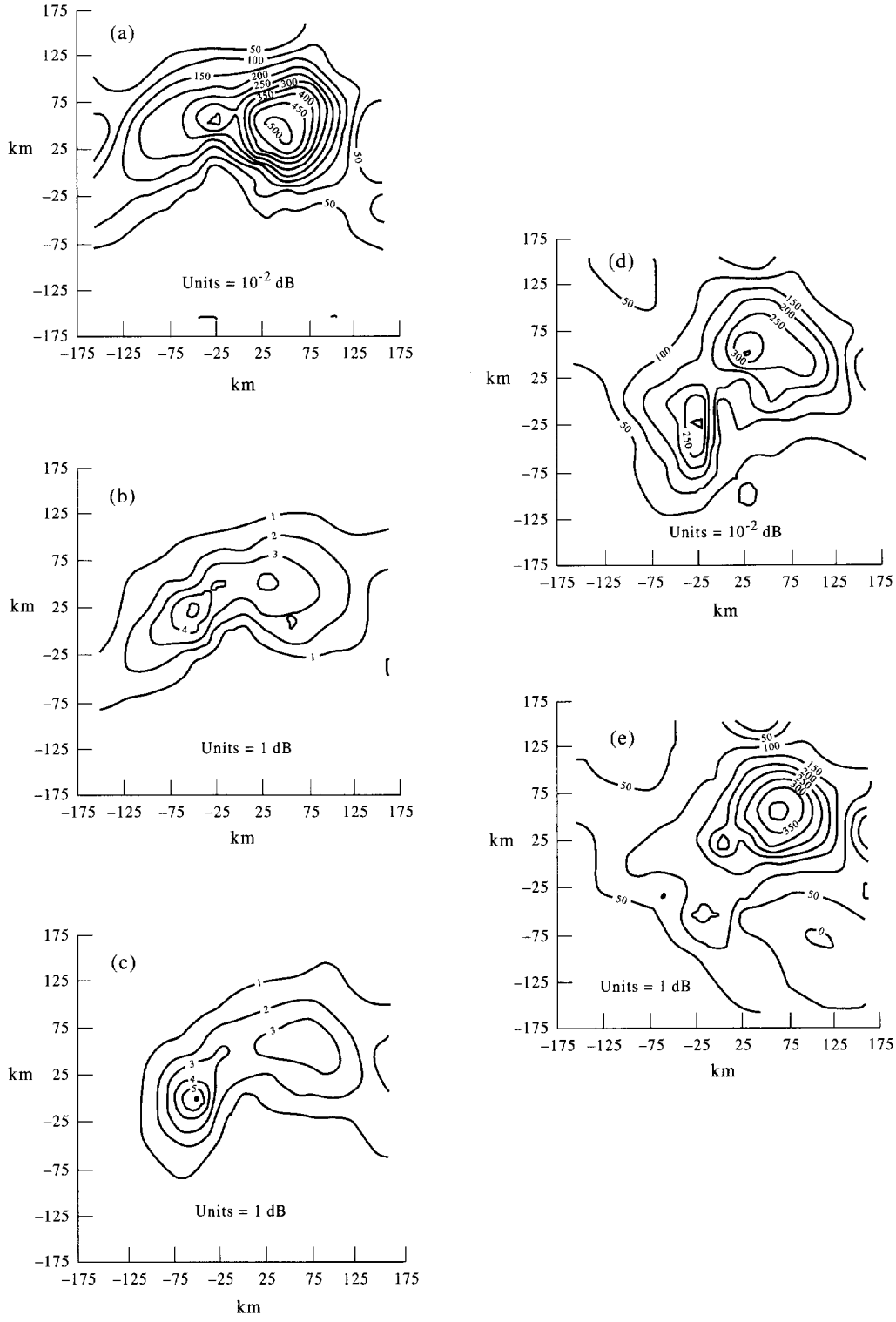

Fig. 10. Sequence of contour plots for South Pole event 89_91 (1 April 1989). These are from 1 s data, and the times are as follows: (a) 2234:39 UT; (b) 2234:47 UT; (c) 2234:55 UT; (d) 2235:09 UT, and (e) 2235:19 UT. Note the similarity between (a) and (e). The whole sequence took only 40 s.

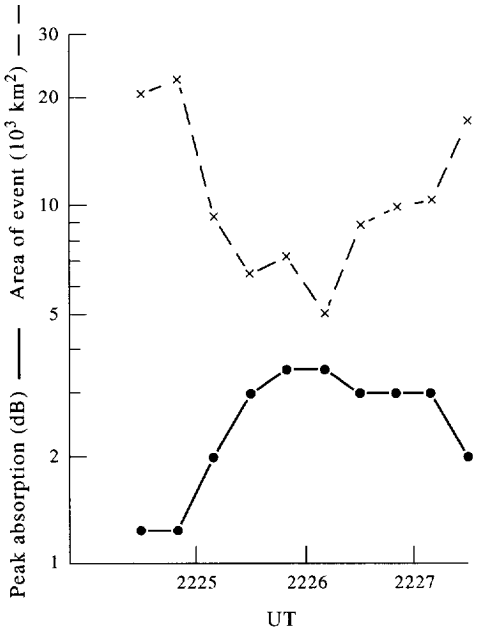

Fig. 11. Area and peak absorption during the growth and decay of a peak of event 89_91.

than the wide-beam instrument. A comparison over the selection of spikes is shown in Table 3, which indicates that ratios may often be as much as 2 or 3.

This result does not necessarily apply to absorption at other times, however. The last part of the event in Fig. 12 is not very different in the first and last panels after 2015 UT, though it reaches the substantial level of 3–4 dB. The reason is that the absorption is more broadly spread during that phase of the event. Although spatial structure is still present, there is also a background at relatively high level, which effectively fills the wide beam at a level up to 3 dB.

A number of comparisons between the readings of wide- and narrow-beam readings at the South Pole have previously been published by Detrick and Rosenberg (1990) and Rosenberg *et al.* (1991). In four comparisons they find ratios of 1.25, 2.33, 5 and 8. It should be appreciated that in a given instance the ratio depends on the position of the event in relation to the centre of the beam, as well as the area covered by the event.

5. DYNAMICS

5.1. *Introduction*

The dynamic character of the spike event was obvious in Fig. 4, and this example is by no means exceptional. Nor is the existence of motion surprising. Several studies using wide-beam riometers, widely spaced, have found that the onset of an absorption event in the night sector moves generally poleward at a relatively high speed, up to several km/s (Hargreaves, 1968; Ranta *et al.*, 1981). The peak of the event is also likely to move, though not necessarily in the same way as the onset. Using a system with four narrow beams at Ramfjord, Nielsen (1980) measured the direction and speed of 14 absorption spikes, showing that their motion was dominantly poleward with speeds ranging from 300 m/s to 3 km/s. The spike often occurs close to the onset, and Nielsen showed that absorption spikes move at the same speed as the poleward border of the radar aurora.

The imaging riometer allows us to study absorption dynamics over distances of 10s of km up to 200 or 300 km, and a number of events have been considered from that point of view both at the Pole and at Kilpisjärvi. We can also address the question of the true duration of the spike event. Before the imaging riometer, it was thought that its apparently short duration (only a minute or two) was probably due to rapid motion over the observing station – e.g. to travel 100 km at 1 km/s takes 100 s. Since the events may now be tracked that question may be resolved.

Table 3. Wide- and narrow-beam absorption

Day	Point, UT	W/B absorption (dB)	N/B	absorption (dB)	Ratio
252	35, 1905:40	2.2	(−1, 2)	6.0	2.7
270	49, 2108:00	0.9	(−1, −1)	3.4	3.8
275	33, 2235:20	1.8	(2, −1)	3.1	1.7
279	42, 2046:50	2.2	(−2, 0)	6.5	3.0
280	164, 1747:10	3.3	(−1, 1)	7.5	2.3
303	102, 1946:50	6.0	(−1, −2)	9.9	1.7
	121, 1950:00	6.4	(−1, −2)	9.4	1.5
	154, 1955:30	10.1	(1, 1)	12.7	1.3
305	59, 2139:40	1.7	(−1, 0)	5.0	2.9
318	67, 1941:00	1.3	(−1, −1)	2.9	2.2
	293, 2018:40	2.3	(0, −2)	5.3	2.3

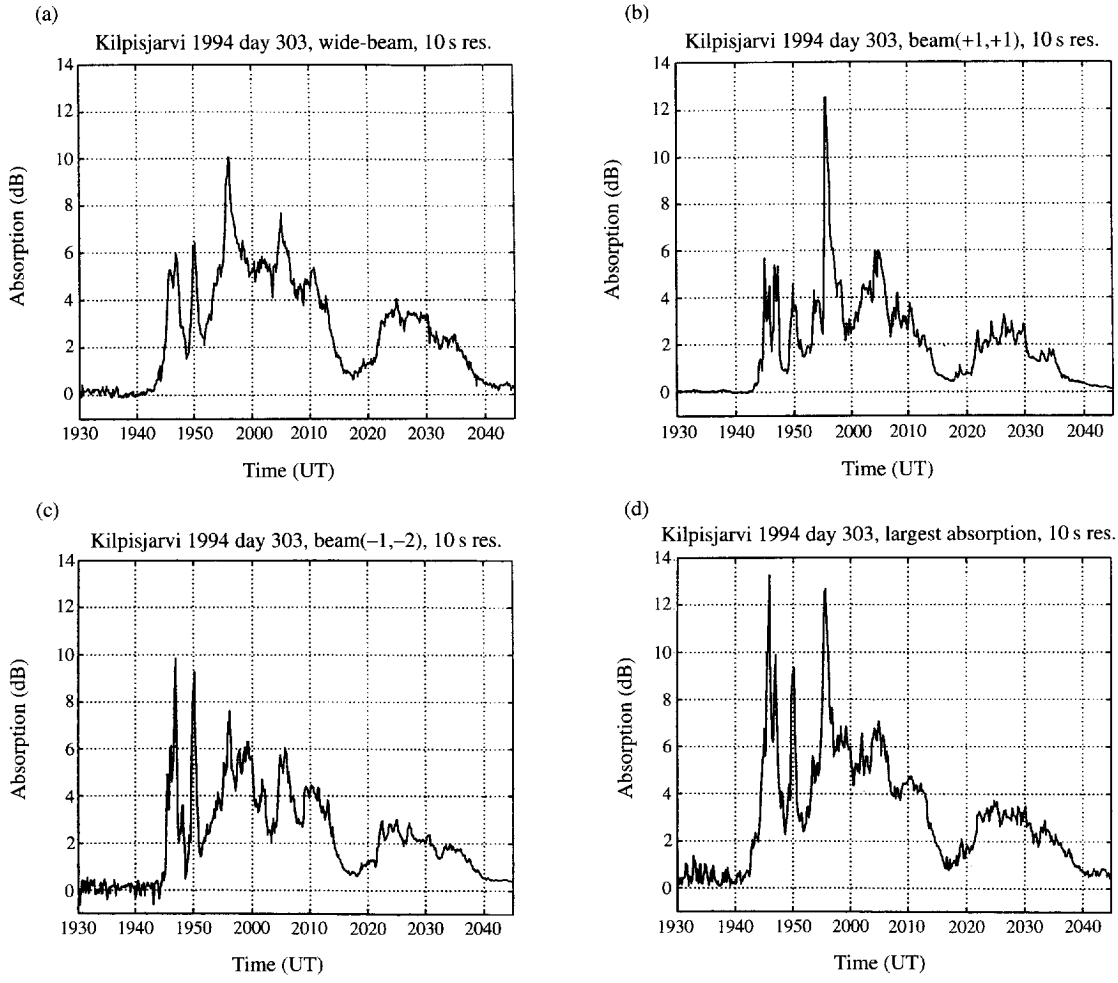

Fig. 12. Response of wide- and narrow-beam riometers during the event on day 303 (30 October 1994) at Kilpisjärvi: (a) Wide beam; (b) IRIS beam (1, 1); (c) IRIS beam (−1, −2); (d) Largest absorption in any IRIS beam. The beams are labelled from overhead (0, 0), positive to the north or east. For example, (−1, −2) is one to the south of overhead and two to the west. With 49 beams, the range of labelling is (±3, ±3).

5.2. *At the South Pole* ($L = 13$)

There is considerable variation from case to case, but there are also some common features. Figure 13 refers to the maximum absorption within the field of view. The first panel shows the magnitude of the maximum absorption, and the second gives the distance of the maximum from overhead in the 'south–north' direction. (At the Pole, this is magnetic south–north, 17 degrees from the normal to the local L shell – see Fig. 8.) There is a clear poleward movement overall, and the average speed over the whole 20 min of the event is 157 m/s. This continues over all six maxima. However, there are significant deviations over shorter periods. Between points 30 and 50 (3.3 min), covering peaks 1–3, there is a temporary poleward excursion of about 50 km. Another occurs over peak 5. The first is further illustrated in Fig. 14(a), which shows the absorption in a south–north section. The example of Fig. 14(b) shows poleward motion at the beginning of an event and equatorward motion towards the end. (Observe the progression of the 0.6 dB contour.) Displays in this format, as well as those like Fig. 13(a) which track the magnitude of

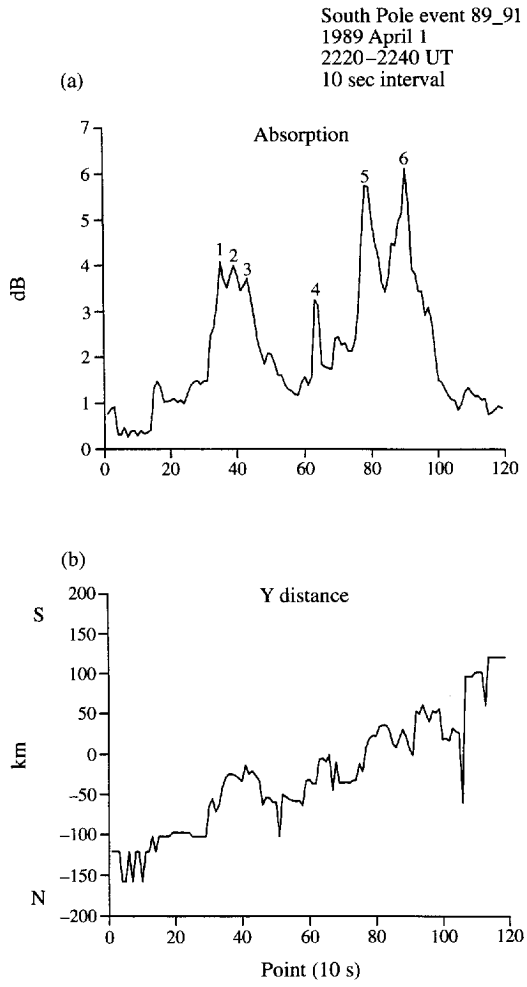

Fig. 13. South Pole event on 1 April 1989 (event 89_91). (a) Maximum absorption (irrespective of the beam in which it occurs). (b) Distance to the maximum in the y (S–N) direction.

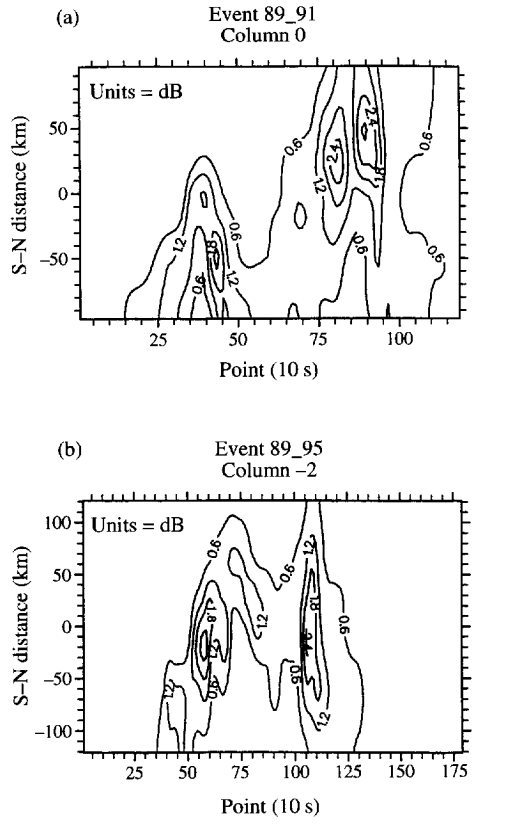

Fig. 14. South–north sections of (a) event 89_91 (1 April 1989), and (b) event 89_95 (4 April 1989) at the South Pole. Each shows poleward and equatorward movements. The activity moved into the field of view from the equatorward side in each case. In (a) it moved away poleward but in (b) it retreated equatorward.

Table 4. Event velocities at the South Pole

Event	Speed to S (m/s)	Speed to E (m/s)	Total speed (m/s)	Direction (E of S)	Duration (min)	Peaks	Distance (km)
88_55	437	586	731	53	5	1–4	219
89_91	157	Osc.	157	—	12	All 6	113
	700	Some	700	—	2	5	84
89_94	523	373	642	35	6	All 4	231
89_95	432	220	485	27	6	1–4	175
	−133	—	133	180	5	After 4	40
89_118	551	917	1070	59	2	Before 1	128
	−192	−433	474	246	8	1–6	228
	−227	−536	582	247	8	7–11	279

the peak from beam to beam, show the actual duration of these short events.

A summary of velocities derived for a number of South Pole events is given as Table 4. Note that east–west components are as large as the north–south ones, giving directions of movement generally south–east or north–west. The number of examples is limited, but so far this line seems not to be the normal to the L shells but some 20–30 degrees from it. The total speed ranges between 157 and 1070 m/s, with median 550 m/s. In this table, the 'duration' is the time over which the velocity was determined, and the 'distance' is the distance covered by the movement. The typical duration of a single spike is, however, only 1–2 min. Despite undulations, there is a clear tendency for the motions to be generally poleward near the start of an event and equatorward near the end. The picture is of an active region arriving from the equatorward side and eventually retreating back towards the equator. Much structure occurs within the active region while it remains within the field of view of the IRIS, the more intense enhancements of which last only for 1–2 min.

5.3. *At Kilpisjärvi* ($L = 5.9$)

The dynamic behaviour at Kilpisjärvi has some similarities with that at the Pole, but the variability is, if anything, even greater. Figure 4 showed an example in which the intense precipitation region moved poleward at about 2 km/s. There was also a substantial eastward component while the spike was at its most intense. But equatorward motions are also seen. In the event of Fig. 15(a), there is a poleward movement during which the spike occurs, followed by an equatorward retreat of weaker absorption, to be followed some 8 min later by a second poleward excursion of weaker intensity not including a spike. Event 318 appeared in the wide-beam riometer (Fig. 2) as a pair of spikes separated by some 40 min. From Fig. 15(b) we see that the first one moved poleward but the second one equatorward.

Table 5 summarizes motions derived from seven Kilpisjärvi events. The 'points' in this Table, being in each case 10 s apart, indicate the period over which the speed was determined. The speeds tend to be greater than those at the Pole. It seems to be the case that spikes at or very close to the start of an event move poleward, whereas those later in the event may very well move in the opposite direction. In this admittedly limited set of data there is no consistency of east–west movement, though it may be similar to the north–south component in magnitude. Note that in the orientations shown in Fig. 8(b), spikes occurring

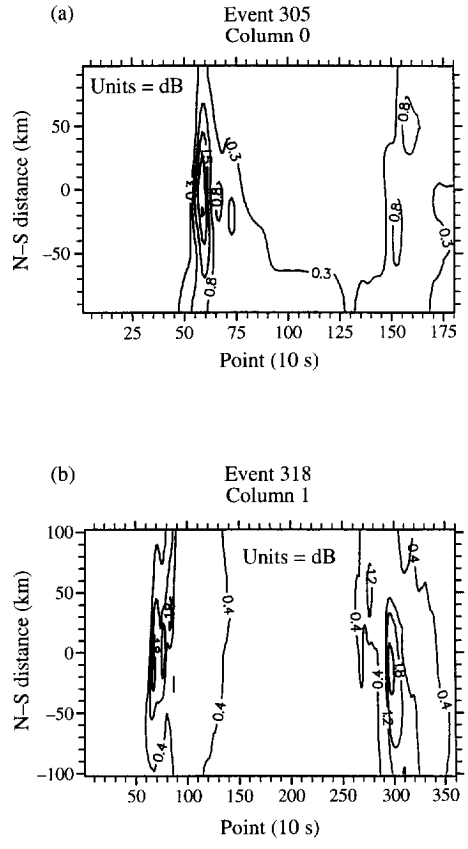

Fig. 15. Poleward and equatorward movements at Kilpisjärvi. (a) Event 305 (1 November 1994). (b) Event 318 (14 November 1994). Compare (b) with the bottom panel of Fig. 2. Of the two spikes seen there, the first moved poleward and the second equatorward.

late and early in the event are tilted in opposite senses from the east–west line.

An earlier study of the direction of movement of absorption events over Alaska (using wide-beam riometers, of course) showed a change of typical direction at $L = 5.5$ (Fig. 16). The present results are consistent with this, and also with the conclusion in that paper that within the first 10 min. of an event most of the absorption features move poleward, but most of the subsequent ones move equatorward.

5.4. *Event duration*

As pointed out above, the imaging riometer, with its ability to track an absorption feature from beam to beam, enables a better resolution to be made between changes in space and time. Table 6 lists the true durations of 12 spikes at Kilpisjärvi, each read to 10 s accuracy between absorption values half the maximum. They range between 40 s and 140 s. In some

Table 5. Motion of absorption patches at Kilpisjärvi

Day	Northward		Eastward	
	Points,	Velocity (m/s)	Points,	Velocity (m/s)
252	30–36,	1560	—	
270	46–58,	908	—	
279	39–48,	2033	39–44,	2167
280	158–167,	−1671	160–167,	614
303	—		85–108,	−765
303	113–126,	−780	—	
305	56–72,	212	—	
318	60–70,	1030	62–86,	−552
	70–90,	reversing		
318	269–289,	−642	—	
	289–323,	slowing		

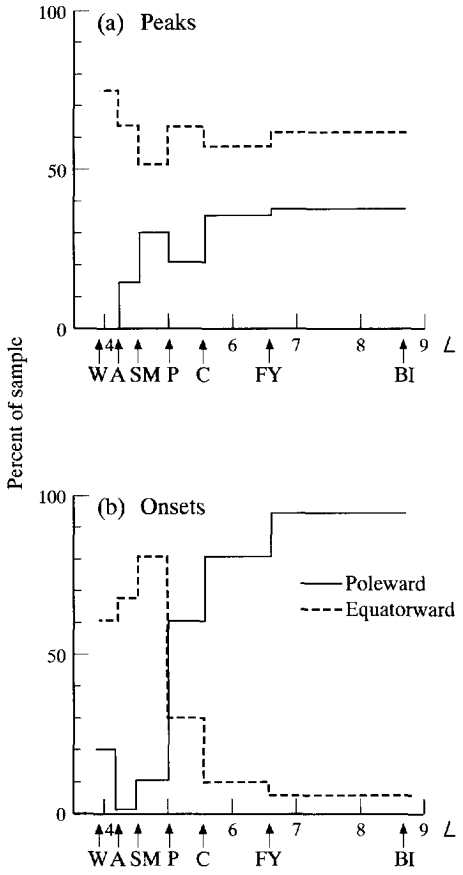

Fig. 16. Relative frequency of poleward and equatorward movements over Alaska for (a) peaks and (b) onsets (Hargreaves, 1974). Note the reversal of typical direction at about $L = 5$.

cases the total speed of the spike was also determined, and then it is possible to state the distance travelled.

Table 6. Duration and travel

Day	Point	Duration	Total speed m/s	Distance km
252	35	80	1560	125
270	49	40	908	36
275	33	140	—	—
279	42,45	60	2970	178
280	164	60	1780	107
303	95	50	765	46
303	121	60	780	47
303	154	110	—	—
305	59	70	212	15
318	86	70	—	—
318	272	120	642	77
318	293	140	—	—

Most of these distances are well within the coverage of the IRIS. Hence, there can be little doubt that these duration values are the true ones, and that each spike travels for only a limited distance. The idea that a short duration is observed because an intense, long-lived, absorption arc has moved rapidly through the beam of the riometer is no longer tenable.

6. OBSERVATIONS OF THE PRECEDING BAY

Some sharp-onset events are preceded by a weak absorption bay lasting as much as an hour. Studies with wide-beam riometers (Hargreaves *et al.*, 1975; Ranta *et al.*, 1981) have shown that this kind of event always moves slowly equatorward and that the substorm appears to evolve from it at some modest latitude (typically $L = 5.5$). The typical behaviour is illustrated in Fig. 17 – the 'reversed-Y event'.

Two examples of pre-onset bays followed by substorm events, as seen with the wide-beam riometer at

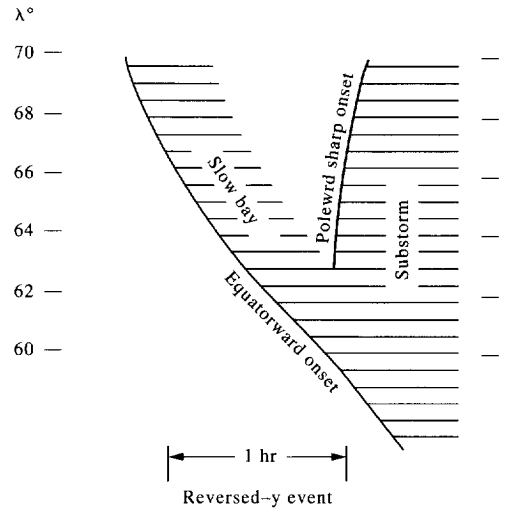

Fig. 17. Idealized reversed-y event, showing the relationship between the equatorward pre-onset bay and the substorm onset (Hargreaves *et al.*, 1975).

Kilpisjärvi, are shown in Fig. 18 The IRIS confirms the arc-like structure and the equatorward drift (Fig. 19). The pictures in this display are at 1 min intervals and the whole covers just over an hour, from 1728 to 1832 UT. The main event began at 1845 UT. It is interesting to note that the arc stretches right across the field of view, essentially east–west, but with some contained structure. Its intensity varies and is strongest towards the end. (However, in other cases the arc has been seen to intensify and fade again before passing out of sight.) The speed of drift in Fig. 19 is 132 m/s over 15 min between 1815 and 1830 UT (more or less the last two rows). The arc moved only very slowly for 30 min before that.

Hargreaves (1975) suggested that the equatorward drift of the preceeding bay might represent an inward $\mathbf{E} \times \mathbf{B}$ drift in the magnetosphere, and gave a formula for the corresponding cross-tail electric field under the (no doubt inaccurate) assumption of dipolar field lines. Table 7 gives the corresponding formula for Kilpisjärvi, the inward speed in the magnetophere and the equivalent electric field, from observation of two drifting bays. The values of electric field are at the lower end of the wide-beam measurements reported by Ranta *et al.* (1981).

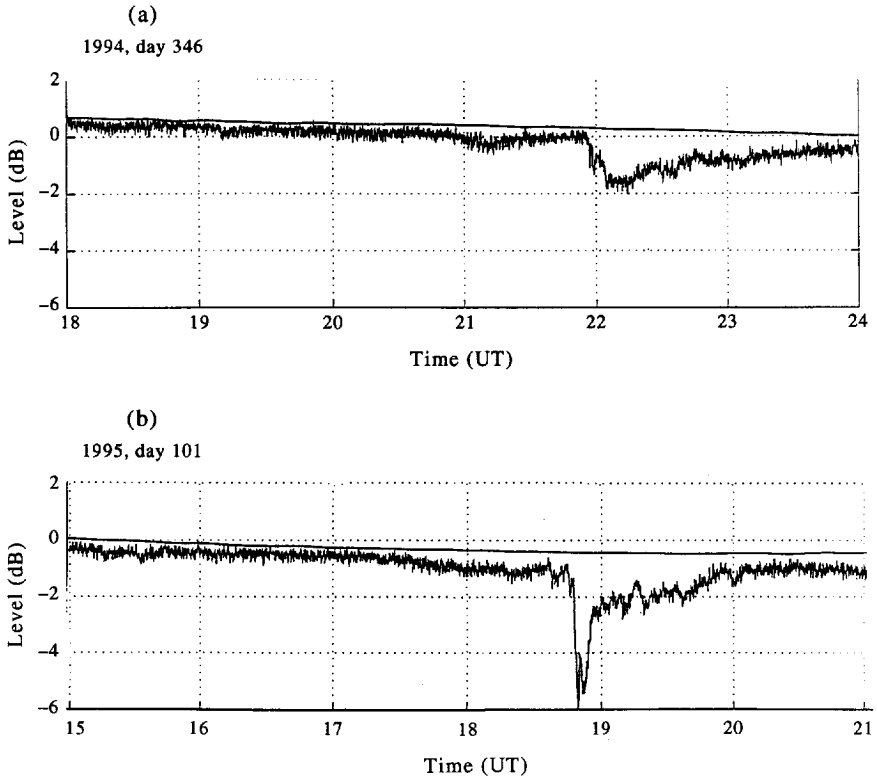

Fig. 18. Examples of preceeding bays at Kilpisjärvi, observed with the wide-beam riometer. (a) Day 346, 12 December 1994. (b) Day 101, 11 April 1995.

Table 7. Equatorward drift at Kilpisjärvi⇒Inward drift in magnetosphere⇒Cross-tail electric field. Assuming $\mathbf{E} \times \mathbf{B}$ drift, $|\mathbf{v}| = |\mathbf{E}|/|\mathbf{B}|$. At equatorial plane, $L = 5.9$, $B = 1.51 \times 10^{-7}$ Wb/m^2. $E = 3.94 \times 10^{-3} . v_{\text{Kilp}}$, where E is in mV/m and v in m/s

Event 346,			
Points 125–145:	$v_{\text{Kilp}} = 122$ m/s	$v_{\text{eq}} = 3.18$ km/s	$E = 0.48$ mV/m
Event 95_101,			
Points 105–135:	$v_{\text{Kilp}} = 8.9$ m/s	$v_{\text{eq}} = 232$ m/s	$E = 0.035$ mV/m
Points 135–150:	$v_{\text{Kilp}} = 132$ m/s	$v_{\text{eq}} = 3.45$ km/s	$E = 0.52$ mV/m

Because of their structure the arcs are not uniformly wide in the north–south plane. These two examples are 60–100 km wide between absorption values which are half the maxixmum value. This means that they move through their own width in about 10 min.

Preceding bays have not been reported from the South Pole.

7. CONCLUSIONS

The properties of absorption spike events are remarkably similar at the auroral station Kilpisjärvi and at the higher latitude of the South Pole. Despite some exceptions, most events are more ellipical in shape than circular or strip-like, with typical dimensions 190×80 km at the lower latitude and 167×74 km at the higher. The major axis lies more along the L shell than across it, though the alignment is not usually exact. The event includes almost the same total magnetic flux at each latitude.

The spikes are dynamic, with typically a poleward motion at the start of an event, and possibly an equatorward motion towards the end. Significant east–west motions also occur. Speeds vary greatly, in the range of a few 100 m/s to a few km/s. Due to the wide total coverage of the imaging riometer the true duration of the spike has been observed as only 1 or 2 min, and its total travel may be observed in many cases. The foregoing properties are fundamental to any description of the mechanism of this intense precipitation event in the night sector.

The effect of the spatial restriction of the event on the reading of a wide-beam riometer has been studied, and it is shown that the absorption is underestimated by as much as a factor of 2 to 3.

It has been verified by direct observation that the slowly moving bay event which often precedes a sharp onset in the night sector has an essentially arc-like form some 60–100 km wide, though with some additional structure. Its speed and intensity may both vary as it drifts equatorward, and it may take an hour to pass across the field of view.

Acknowledgements—The imaging riometer project at Kilpisjärvi is a joint project between the Engineering Department of the University of Lancaster, funded by the UK Particle Physics and Astronomy Research Council, and the Sodankylä Geophysical Observatory. The work by the University of Maryland at the South Pole is supported by the US National Science Foundation (grants OPP-9119753 and OPP-9505823). The assistance of Dr. A. Phillips and M. C. Rose of the British Antarctic Survey, Cambridge, P. Villeki of the Sodankylä Geophysical Observatory, and R. O. Mackin from Lancaster during the installation at Kilpisjärvi is gratefully acknowledged. We thank K. Ranta for operating the equipment at Kilpisjärvi and the Finnish Forest Service for permission to use the site.

REFERENCES

Detrick D. L. and Rosenberg T. J. 1990 A phased-array radiowave imager for studies of cosmic noise absorption. *Radio Sci.* **25,** 325.

Hargreaves J. K. 1968 Auroral motions observed with riometers: latitudinal movements and a median global pattern. *J. atmos. terr. Phys.* **30,** 1461.

Hargreaves J. K. 1974 Dynamics of auroral absorption in the midnight sector – the movement of absorption peaks in relation to the substorm onset. *Planet. Space Sci.* **22,** 1427.

Hargreaves J. K., Chivers H. J. A. and Petlock J. D. 1964 A study of auroral absorption events at the South Pole. *J. geophys. Res.* **69,** 5001.

Hargreaves, J. K., Chivers H. J. A. and Axford W.I. 1975 The development of the substorm in auroral radio adsorption. *Planet. Space Sci.* **23,** 905.

Hargreaves, J. K., Chivers H. J. A. and Nielsen, E. 1979 Properties of spike events in auroral radio adsorption. *J. geophys. Res.* **84,** 4245.

Hargreaves J. K., Detrick D. L. and Rosenberg T. J. 1991 Space–time structure of auroral radio absorption events observed with the imaging riometer at South Pole. *Radio Sci.* **26,** 925.

Nielsen E. 1980 Dynamics and spatial scale of auroral absorption spikes associated with the substorm expansion phase. *J. geophys. Res.* **85,** 2092.

Nielsen E. and Axford W. I. 1977 Small-scale auroral absorption events associated with substorms. *Nature* **267,** 502.

Parthasarathy R. and Berkey F. T. 1965 Auroral zone studies of sudden onset radio wave absorption events using multiple-station and muliple-frequency data. *J. geophys. Res.* **70,** 89.

Ranta H., Ranta A., Collis P. N. and Hargreaves J. K. 1981 Development of the auroral absorption substorm: studies of pre-onset phase and sharp onset using an extensive riometer network. *Planet. Space Sci.* **29,** 1287.

Rosenberg T. J., Detrick D. L., Venkatesan D. and van Bavel G. 1991 A comparative study of imaging and broad-beam riometer measurements: the effect of spatial structure on the frequency dependence of auroral absorption. *J. geophys. Res.* **97,** 17793.

Stauning P. and Rosenberg T. J. 1996 High-latitude daytime absorption spike events. 1. Morphology and occurrence statistics. *J. geophys. Res.* **101,** 2377.

Taylor C. M. 1986 A catalogue of spike events observed at Abisko, Sweden, 1 August 1979–31 July 1986. Environmental Sciences Report TR/41, University of Lancaster.